ORIGINAL ARTICLE
Electrica 2026; 26: 1-14

Experimental Investigations on Improving the Accuracy of MTPA Strategy by Considering System Nonlinearities in Practical IPMSM Drives for Electric Vehicle

Osman Emre Özçiflikçi[1,2], Mikail Koç[3], Serkan Bahçeci[4]

[1]Department of Electrical-Electronic Engineering, Kırşehir Ahi Evran University Faculty of Engineering-Architecture, Kırşehir, Türkiye
[2]Department of Electrical-Electronic Engineering, Erciyes University Graduate School of Natural and Applied Sciences, Kayseri, Türkiye
[3]Department of Electrical-Electronic Engineering, Kırşehir Ahi Evran University Faculty of Engineering-Architecture, Kırşehir, Türkiye
[4]Department of Electrical-Electronic Engineering, Erciyes University Faculty of Engineering ,Kayseri, Türkiye

Cite this article as: O. E. Özçiflikçi, M. Koç and S. Bahçeci, "Experimental investigations on improving the accuracy of MTPA strategy by considering system nonlinearities in practical IPMSM drives for electric vehicle," *Electrica*, 2026, 26, 0181, doi: 10.5152/electrica.2026.25181.

WHAT IS ALREADY KNOWN ON THIS TOPIC?

- *MTPA control is widely used in IPMSMs to provide efficient control. However, most existing methods are model-based and parameter-dependent. Conventional techniques are susceptible to nonlinear system characteristics such as magnetic saturation, which negatively affect torque control accuracy.*

Corresponding author:
Osman Emre Özçiflikçi

E-mail:
osman.ozciflikci@ahievran.edu.tr

Received: June 13, 2025
Revision Requested: September 11, 2025
Last Revision Received: October 13, 2025
Accepted: October 20, 2025
Publication Date: January 29, 2026

DOI: 10.5152/electrica.2026.25181

ABSTRACT

Interior mounted permanent magnet synchronous machines (IPMSMs) are commonly preferred by electric vehicle manufacturers due to their reluctance torque production capability, high efficiency, and so on. The use of the maximum torque per ampere (MTPA) strategy, which allows maximizing the torque production in IPMSMs, is mandatory for high efficiency operation in the constant torque region. However, the parameters used in the implementation of the MTPA strategy significantly vary depending on the operating conditions. Although the improvement of the MTPA strategy by addressing parameter variations is widely discussed in the literature, mostly errors occur in the production of command currents due to the neglected partial derivatives of the parameters with respect to the current angle. Besides, high-fidelity machine models are not provided by the manufacturer in most commercial machines. This article presents a method for determining MTPA points in IPMSMs in real time. Even without prior knowledge of machine parameters, accurate MTPA can be obtained through focused experimental testing.

Index Terms—Advanced torque control, improved lookup table, maximum torque per ampere (MTPA), parameter variations

I. INTRODUCTION

The increasing use of conventional energy sources causes global warming and worrying environmental problems such as acid rain. Transportation is a dominant sector where energy consumption is quite high [1]. Electric vehicles play an important role in contributing to society as they facilitate the use of clean energy technologies such as solar, wind, biomass, etc. Permanent magnet synchronous machines (PMSM) are widely used in electric vehicle applications due to their superior features such as high power/torque density, high efficiency, and low acoustic noise, and so on [2-10]. It is evident in [2] that as of 2010, the rate of PMSM usage in electric vehicles produced by widely used brands such as Hyundai, BMW, Volkswagen, Renault, Tesla, and Nissan is higher than other machine types. In [11], a detailed research has been carried out in terms of the use of different machine types in electric vehicles, and it has been stated that interior mounted PMSM (IPMSM) is used in Nissan Leaf, Soul EV, and Toyota Prius brand vehicles, and its efficiency is higher than brushless direct current (DC) motor (an alternating current (AC) machine in fact), switched reluctance motor, and induction motor. Hence, IPMSMs are quite commonly preferred [12].

In electric vehicles, the accelerator pedal is the torque command of the system. Drivers adjust the speed of the vehicle based on their desire, and torque control is expected from the machine. In fact, regardless of the system input, whether it is the position or the speed command, it is essential that stable torque control with high efficiency operation must be achieved in either

WHAT THIS STUDY ADDS ON THIS TOPIC?

- *This study proposes an experimental, parameter-independent MTPA approach that directly accounts for the nonlinear characteristics of the system by determining the optimal operating points. The resulting look-up table (LUT) provides accurate and reliable torque control without the need for machine parameters.*

case. Therefore, the precise generation of torque control and current commands is critical for PMSMs employed in electric vehicles. Since only magnet torque is used in surface mounted PMSM (SPMSMs), the most efficient operation is achieved by setting the -d axis current command to zero. Unlike SPMSMs, the most efficient control is achieved by performing maximum torque per ampere (MTPA) control by altering both −dq axis currents in IPMSMs rather than $I_d = 0$ control [13-16]. With the use of the MTPA strategy, a serious improvement in the drive efficiency can be achieved. One of the commonly used methods for MTPA implementation is based on finding MTPA points through mathematical analysis. The higher-order equation obtained by differentiating the electromagnetic torque value with respect to the β angle is generally solved by the Newton–Raphson iteration method. Another commonly used method for the MTPA strategy is to apply command currents to the drive system through previously obtained and stored lookup tables [17]. Since solving mathematical equations while the machine is in operation increases the computational burden on the microprocessor, the burden is much reduced by using lookup tables [1]. Methods such as search, real signal injection, and virtual signal injection–based MTPA implementation are also common. In practical implementations, however, search methods may have stability issues in rapid load changes, real signal injection methods increase losses because a real signal is injected into the drive system, and acoustic noise may also appear [18], and the virtual signal injection method may still be model-dependent, as in [19]. Furthermore, any kind of signal injection techniques, regardless of real or virtual injection, increase total harmonic distortion (THD), and hence the torque ripple increases in a real-world drive [20]. Hence, numerical solutions and lookup table methods are still attractive and frequently employed in the implementation of the MTPA strategy. However, the use of numerical methods or lookup tables may still be vulnerable to parameter variations in practice [1, 21]. It is evident in the literature [22] that either online or offline numerical solutions of the stator current angle (β angle) do not give optimum current angle in practice since partial derivatives of the machine parameters with respect to current angle are not considered [23]. Since L_d, L_q, and Ψ_m are used in such drives, deviations occur in the production of command currents from their accurate values. Hence, the drive cannot actually produce the correct commands due to variations in the machine parameters in real life, and this results in reduced drive efficiency. This issue, in fact, is the main concern of this paper.

If the works in which MTPA has been developed by parameter estimation are reviewed, in [24], the controller of the IPMSM has been improved to enhance command accuracy in constant torque and constant power regions by accurately estimating the −dq axis inductances and stator resistance. However, variations in the magnetic flux linkage, which play a dominant role in torque production, have been neglected. Similarly, in [25], −dq inductance values are estimated online and used in MTPA equations with the model reference adaptive system (MRAS) technique to improve MTPA against parameter variations. However, since the partial derivative expressions of the parameters have been neglected, improving MTPA with parameter estimation techniques does not allow the drive to operate at an accurate MTPA trajectory, as evident in [22]. Additionally, the magnet flux linkage variation is ignored in [25]. In [26], researchers aim to improve the MTPA strategy by estimating L_q and Ψ_m values with the MRAS technique, with conventional MTPA equations in which the partial derivative terms of the parameters are not considered. However, since the current angle β is calculated with conventional equations, accurate control cannot be achieved. In addition, in numerical parameter estimation methods as in [27], the signal injection needs to be applied to the parameters L_d, L_q, and Ψ_m for correct estimations due to the rank deficiency issue. Since the rank of the −dq axis equations is two, it is possible to estimate only two parameters. There are also studies in the literature in which sinusoidal signals are injected to avoid the rank deficiency problem and to estimate the parameters accurately [21, 27]. However, parameter estimation with such signal injection techniques has some practical issues as discussed above, and still may not be able to accurately detect the MTPA points.

The machine parameters are used in the implementation of MTPA strategies with direct voltage calculation in recent years [28-31]. [28, 29] emphasizes that the two current control loops required for field oriented control (FOC) can be operated with a single voltage control loop, and a simpler drive system can be obtained. In fact, a much simplified MTPA strategy based on direct voltage calculation has been investigated in [28] without using current sensors. However, direct voltage calculation-based MTPA studies involve complex numerical calculations, and the use of machine parameters is also dominant. It is, therefore, questionable whether MTPA points can be obtained with high accuracy due to inevitable variation in machine parameters. Similar to studies in [28, 29], the direct voltage MTPA technique is also performed in [30, 31], and clearly, these drives are vulnerable to parameter variations as well. Different techniques have also been

reported in the literature to make conventional MTPA strategies robust to parameter variations [23, 32-35]. In [32], the determination of the MTPA current angle via speed harmonics is discussed. Adding harmonic voltages to the reference voltages at PI (proportional and integral) outputs increases the computational burden and complexity. Further, the problems associated with signal injection techniques arise. In [23], an MTPA strategy is proposed considering partial derivative expressions of the machine parameters with the virtual signal injection technique. However, the drive, in fact, is still vulnerable to the –d axis inductance variation. Therefore, the MTPA implementation strategy has been further improved in [33] by estimating the -d axis inductance with the MRAS technique. However, the easier implementation without complex control algorithms and avoiding high burden on the processor are not less important design challenges where [33] suffers. In [34], the optimum reference flux value for MTPA is determined with the search method by applying the extreme seeking control technique in an IPMSM drive with direct torque control. Although a parameter-independent MTPA strategy has been developed, the issues associated with the complexity of the filter designs and the difficulty of adaptation to drives with other control techniques, such as FOC, arise. In [35], an MTPA study is carried out with a search-based perturb and observe strategy, where issues pertinent to search algorithms may arise, such as the stability problem. In [36, 37], the authors proposed 2D-LuT-based MTPA. Ψ_m variations are considered with a flux observer structure, and the results validate improvement. However, the drives do not consider magnetic saturations and hence are vulnerable to inductance variations. It is well-known in the literature that –dq axis inductances vary considerably with the current magnitude. There are also studies that compare different MTPA strategies with each other and comprehensively review the literature [38-42].

The main contribution of this study is to highlight that the MTPA trajectory of an IPMSM can change in real time due to parameter variations and inverter nonlinearities in the conventional lookup table obtained using the Finite Element Method during the design phase. The proposed method enables the determination of optimal MTPA points even in commercial machines with unknown or unavailable parameters. To this end, online tests have been performed on an FOC-based IPMSM drive to identify the points where the actual torque is maximized under constant stator current and varying current angle conditions. Conventional MTPA strategies based on lookup tables are typically created using nominal parameters or ideal mathematical models, and these models may not capture parameter variations or inverter nonlinearities. In contrast, the proposed method adapts directly to actual operating conditions without requiring any stored parameter information. The effectiveness of the strategy has been compared with conventional Newton–Raphson-based MTPA and validated on a 4.1 kW prototype IPMSM machine test system. This paper provides a practical and highly accurate methodology for researchers interested in controlling motors designed by others.

II. MATERIAL AND METHODS

In this study, it is aimed to implement the MTPA strategy on a FOC-based drive. Mathematically, Clark and Park transformations are used for the coordinate transformations in FOC-based drives. Among pulse width modulations, space vector pulse width modulation (SVPWM) is preferred in the drive due to its superior features, such as lower switching losses and less current distortion [43].

A. Interior Mounted Permanent Magnet Synchronous Machine Modeling

With Clark and Park transformations, the IPMSM –dq frame can be modeled as in (1–8) [27]. The schematic of the proposed IPMSM drive is given in Fig. 1. A voltage limitation block is used in the drive for voltage constraint (with circle limitation strategy) since the battery usage rate is $V_{dc}/\sqrt{3}$ for the SVPWM technique.

$$V_d = R^* I_d + \frac{d\psi_d}{dt} - \omega^* \psi_q \quad (1)$$

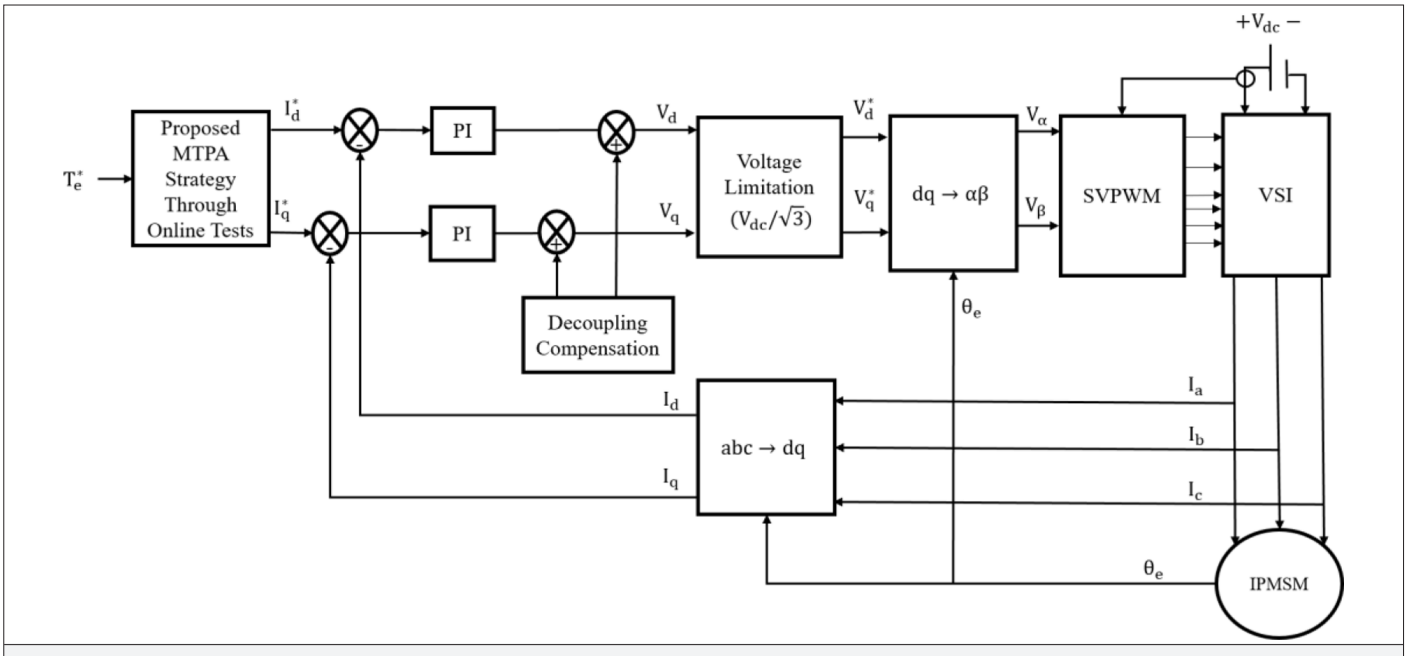

Fig. 1. Proposed interior mounted permanent magnet synchronous machine drive.

$$V_q = R*I_q + \frac{d\psi_q}{dt} + \omega*\psi_d \quad (2)$$

$$\psi_d = \frac{1}{s}\left[V_d - R*I_d + \omega*\psi_q\right] \quad (3)$$

$$\psi_q = \frac{1}{s}\left[V_q - R*I_q - \omega*\psi_d\right] \quad (4)$$

$$I_d = \frac{\psi_d - \psi_m}{L_d} \quad (5)$$

$$I_q = \frac{\psi_q}{L_q} \quad (6)$$

$$T_e = \frac{3*p}{2}\left[\psi_m*I_q + (L_d - L_q)I_d*I_q\right] \quad (7)$$

$$\omega_m = \int \frac{T_e - T_m - B*\omega_m}{J} * dt \quad (8)$$

V_d and V_q represent the voltage values (Volt) on the axes, I_d and I_q represent the current values (Ampere), and Ψ_d and Ψ_q represent the flux values (Weber). ω represents the electrical angular speed value (rad/s), L_d and L_q represent the inductance value (Henry) on the -d and -q axes, Ψ_m represents the magnet flux linkage (Weber). T_m in the mechanical equations represents the load torque (Nm) in the machine, J represents the inertia (kg m^2), and B represents the friction coefficient.

B. Conventional Newton–Raphson–Based Maximum Torque Per Ampere Solution for Torque Control

I_d and I_q currents are the vector components of the stator current I_s:

$$I_d = -I_s * \sin\beta \quad (9)$$

$$I_q = I_s * \cos\beta \quad (10)$$

$$|I_s| = \sqrt{I_d^2 + I_q^2} \quad (11)$$

I_s represents the stator current vector and β represents the angle of the optimum stator current. Equations (9–11) are written in place of (7), and the point where the derivative of the torque value with respect to the current angle is equal to zero is found to find the optimum operating point. The torque equation and derivative expressions are given in (12, 13).

$$T_e = \frac{3*p}{2} * (\psi_m * I_s * \cos\beta + (L_q - L_d) * I_s^2 * \sin\beta * \cos\beta) \quad (12)$$

$$\frac{dT_e}{d\beta} = \frac{3*p}{2}[-\psi_m * I_s * \sin\beta + (L_q - L_d) * I_s^2 * \cos 2\beta] \quad (13)$$

The value of the β angle is found by equating the derivative expression in (12, 13) to zero. The β angle obtained by assuming that the machine parameters are constant is as in (14).

$$\beta = \sin^{-1}\left(\frac{-\psi_m + \sqrt{\psi_m^2 + 8*(L_q - L_d)^2 * I_s^2}}{4*(L_q - L_d)*I_s}\right) \quad (14)$$

If (9–11) are written in their place in (12, 13) and solved according to the I_d current, (15) is obtained.

$$I_d = \frac{\psi_m}{2*(L_q - L_d)} - \sqrt{\frac{\psi_m^2}{4*(L_q - L_d)^2} + I_q^2} \quad (15)$$

If (15) is written in place of the torque equation and solved, the function of the axis current I_q given by (16) is found.

$$(L_q - L_d)^2 * I_q^4 + \frac{2*T_e}{3*p} * \psi_m * I_q - \left(\frac{2*T_e}{3*p}\right)^2 = 0 \quad (16)$$

Since the current function I_q is a 4th-order nonlinear function, the Newton–Raphson iteration method can be used to solve nonlinear functions. The solution equation of the Newton–Raphson method is given in (17).

$$f(n+1) = f(n) - \frac{f(n)}{f'(n)} \quad (17)$$

If the derivative of the current function I_q is taken, (18) is obtained.

$$4*(L_q - L_d)^2 * I_q^3 + \frac{2*T_e}{3*p} * \psi_m = 0 \quad (18)$$

In order to start the Newton–Raphson iteration, the initial value of the I_q current must be determined. Equation (19) is used to calculate this value.

$$I_q^{MTPA}(0) = \frac{2*T_e}{3*p*\psi_m} \quad (19)$$

After finding the optimum value of the I_q current, the value of the I_q current is written in place of the torque equation for the optimum value of the I_d current, and the reference value for the I_d current is produced. The formula for the optimum value of the I_d current is given in (20).

$$I_d^{MTPA} = \frac{2*T_e}{3*p*I_q^{MTPA}*(L_d - L_q)} - \frac{\psi_m}{(L_d - L_q)} \quad (20)$$

The flowchart for Newton–Raphson-based MTPA control, created using ideal parameters for the torque control of IPMSM, is given in Fig. 2.

While the relationship between –dq axis currents and stator current is given by (9, 10), the equation conventionally used in MTPA application is given by (14). Equation (14) is solved by numerical methods in conventional drives in order to find the alleged optimum value of the current angle β shown in Fig. 3, and generally, the Newton–Raphson iteration technique is employed [13]. After obtaining the current angle, –dq axis command currents are generated, and the MTPA strategy is designed. However, (14) used in β calculation is not practically accurate due to the nonlinear behavior of the parameters [23, 39]. Therefore, it is impossible to guarantee the accurate MTPA trajectory operation in those drives where (14) is utilized for command current generation. The severity of the issue has been proven in [23]. Many state-of-the-art drives suffer from the issue as elaborated in the Introduction, and the proposed

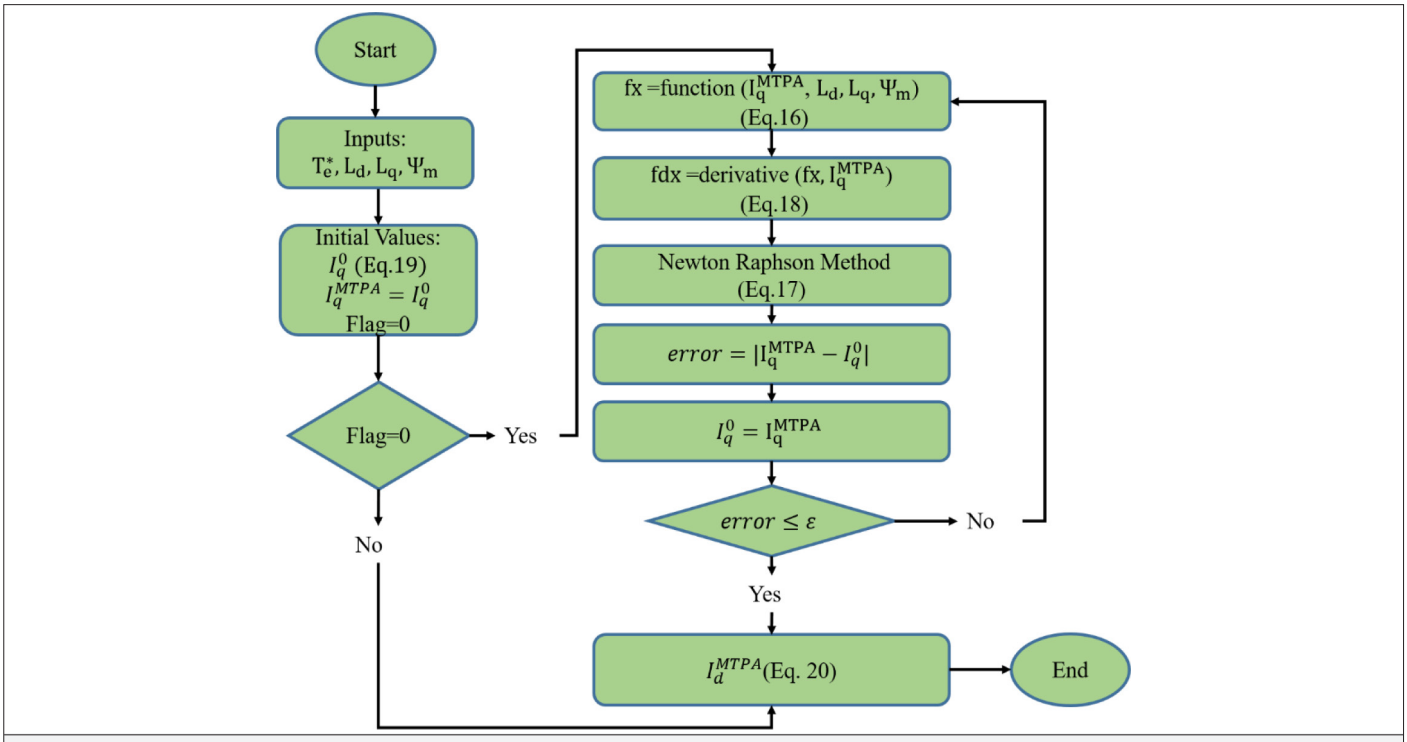

Fig. 2. Flowchart of Newton–Raphson-based maximum torque per ampere strategy.

approach to detect accurate MTPA trajectory offers a simple and robust technique for high-efficiency operation. The given conventional Newton–Raphson equations work correctly when an ideal machine is used. However, when system variations are taken into account, it is seen that the β, I_d, and I_q values produced may be incorrect.

The prototype IPMSM is shown in Fig. 4. Based on (7) and the above modeling equations, MTPA curves of the prototype machine, obtained with the Newton–Raphson-based solution in the ideal case, are given in Fig. 5. Accordingly, the –dq axis currents where the machine will produce up to 5 Nm torque are roughly –18 A and 30 A, respectively. In fact, the MTPA results solved with the conventional Newton–Raphson method can ideally be used with the lookup table or online solution of numerical equations as given in Fig. 5.

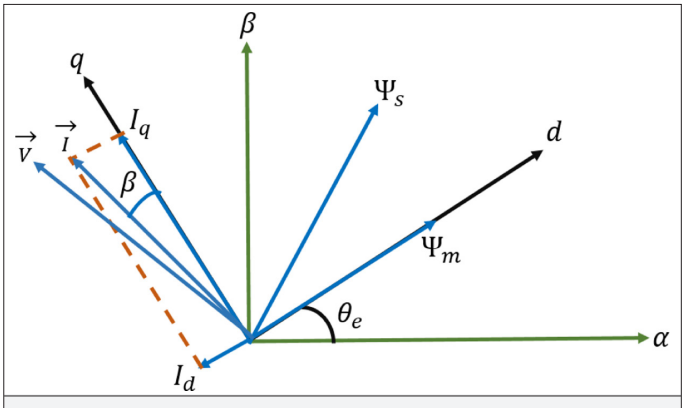

Fig. 3. Current, voltage, and stator flux vectors in stationary and rotating frames.

III. SIMULATION RESULTS

Considering that torque control is important in electric vehicles, 5 Nm torque has been demanded from the ideal drive under varying speed conditions. The specifications of the machine used to obtain the simulation results are given in Table 1. In Fig. 6, system validation is carried out by monitoring demand electromagnetic torque, mechanical speed, –dq axis currents, β angle, and stator current magnitude values. The input power, output power, and efficiency can be obtained by (21–23) [1]. It can be seen from Fig. 6 that the drive successfully controls the torque in both the steady states and transient states at low and high speeds. By comparing Fig. 5 and Fig. 6, one can deduce that the MTPA strategy produces the correct command currents and the drive works efficiently, regardless of the speed in response to the 5 Nm torque demand. This is as expected since, theoretically, the MTPA strategy is independent of speed in the constant torque region. The switching frequency for SVPWM is set to 8 kHz, while obtaining the simulation results, and the command currents are generated by Newton–Raphson iteration technique as detailed in [1].

$$P_{in} = \frac{3}{2} * \left(V_d * I_d + V_q * I_q \right) \quad (21)$$

$$P_{out} = w_m * T_e \quad (22)$$

$$\%\eta = \frac{P_{out}}{P_{in}} * 100 \quad (23)$$

The cutoff frequency (w_c) is determined according to the equations given between (24–26), and the PI parameters are determined to provide control. w_c represents the cutoff frequency, K_{p-d} and K_{p-q} represent the d and q axis proportional coefficients, and K_I is the integral coefficient.

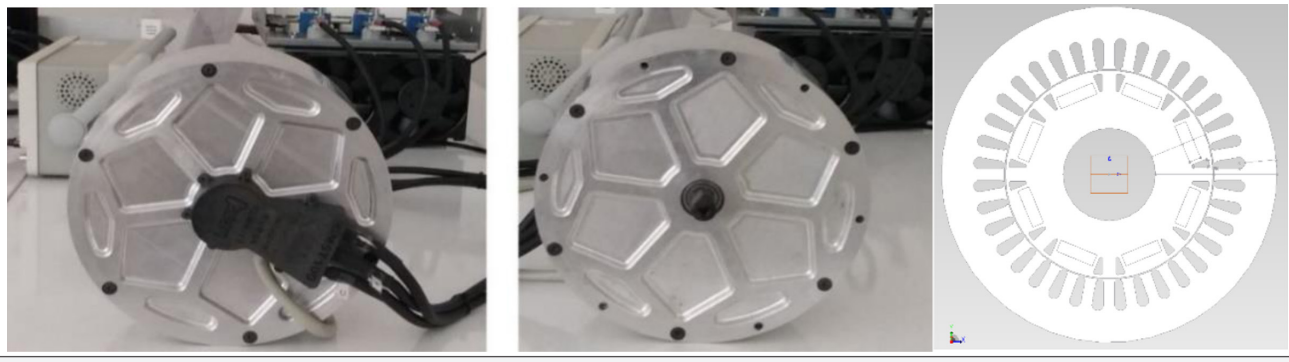

Fig. 4. Prototype interior mounted permanent magnet synchronous machine image.

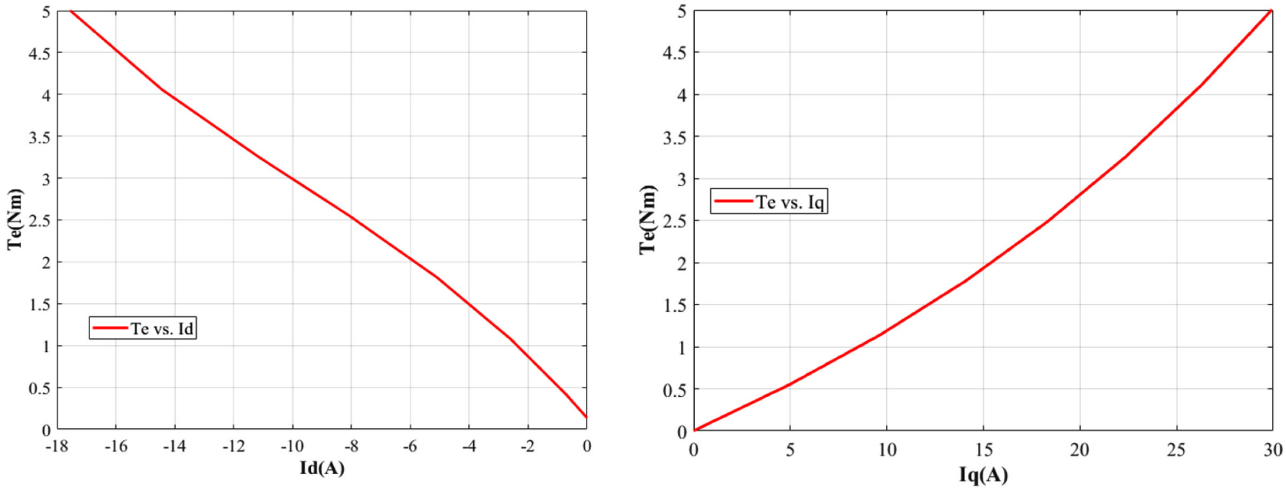

Fig. 5. Optimum –dq axis currents for an ideal machine.

$$K_{p-d} = L_d * w_c \quad (24)$$

$$K_{p-q} = L_q * w_c \quad (25)$$

TABLE 1. INTERIOR MOUNTED PERMANENT MAGNET SYNCHRONOUS MACHINE SPECIFICATIONS

Type	IPMSM
Number of phase	3
Number of pole pairs	4
Continuous torque	15.7 Nm
Continuous power	4.1 kW
–dq Axis inductances	L_d=0.282 mH, L_q=0.828 mH
Flux linkage	φ_m= 0.0182 Wb
Stator resistance	R_s=0.0463 Ω
Inertia	J=0.0071572 kg*m^2
Input voltage range	12 V–600 V

IPMSM, interior mounted permanent magnet synchronous machine.

$$K_I = R * w_c \quad (26)$$

Fig. 6 validates that stable torque control is achieved when an ideal machine behavior is represented in simulations. However, it is evident in [44] that the actual values of L_d, L_q, and Ψ_m parameters of an IPMSM machine at full load operation can be ~30%, ~50% and ~25%, respectively, lower than that of their actual values at no load operation. This implies that the influence of machine parameter variation cannot be ignored in practical implementations if efficiency is of concern. The prototype machine shown in Fig. 4 has been designed to achieve a production of 15.7 Nm continuous torque. Thus, based on the typical variation rates discussed above, the simulated drive has been deliberately operated considering 10%, 16.5%, and 8% reduced L_d, L_q, and Ψ_m, respectively, at 5 Nm electromagnetic torque command. It is noteworthy that the machine parameters are altered in the simulated drive, while the nominal parameters remain the same in the controller as in real-life experiments. It is clear from Fig. 7 that the demand torque cannot be produced when nominal parameters are employed in the MTPA strategy.

As can be seen from Fig. 7, if the variation in the parameters used in the calculation of the MTPA strategy is not considered in the controller, a gap occurs between the actual torque and the demanded torque. Considering electric vehicle applications specifically, failure to meet the torque demanded by the drive will lead to decreased

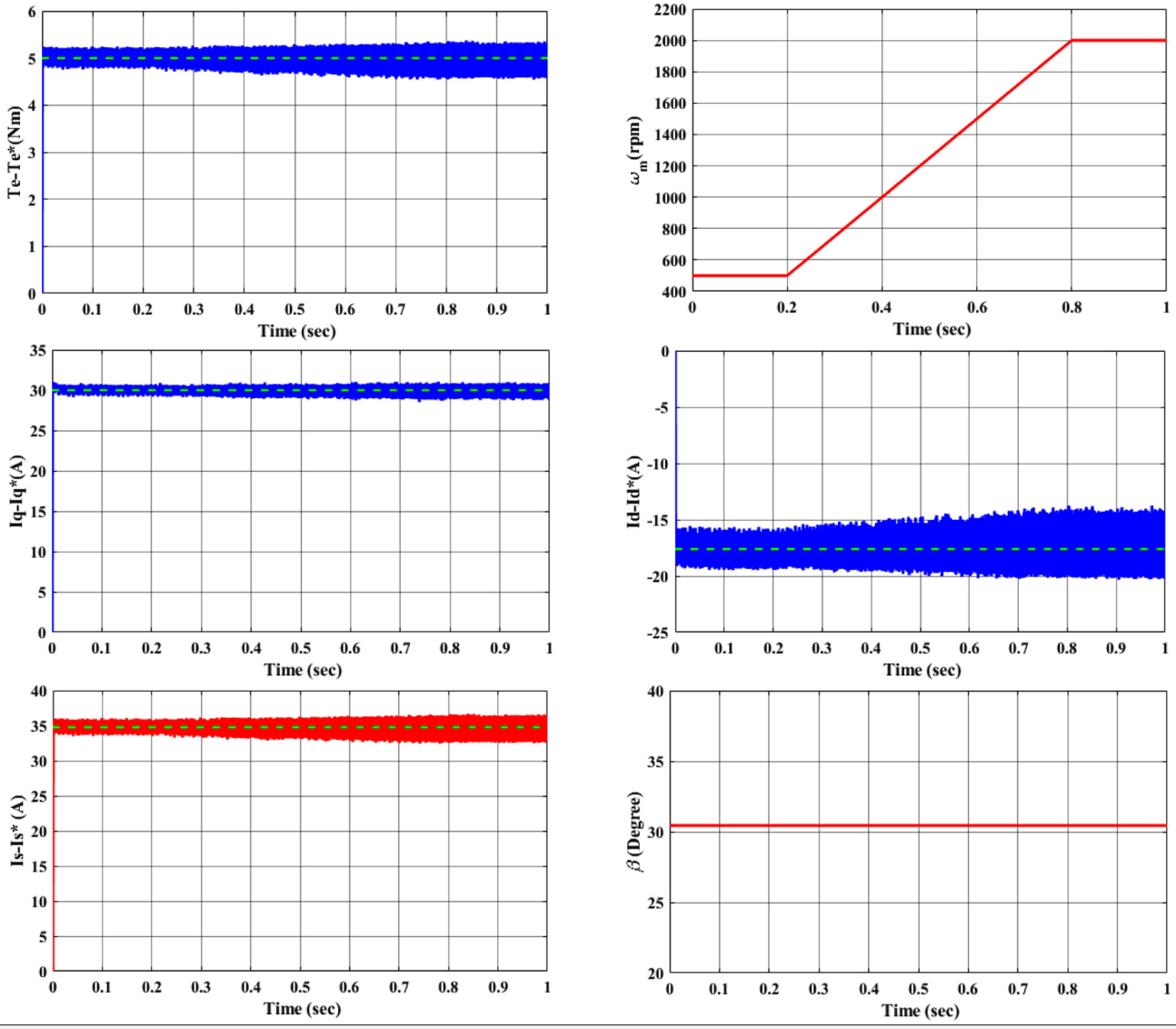

Fig. 6. Validation of field oriented control–based interior mounted permanent magnet synchronous machine drive with conventional maximum torque per ampere strategy.

performance and efficiency in the vehicle. Regardless of the speed, accurate torque control cannot be achieved unless the current commands are generated considering parameter variations. Moreover, compensating the MTPA strategy by employing accurate parameters in (14) is not an exact solution in finding the correct MTPA points [45]. This implies that obtaining the optimum β angle utilizing (14) will not achieve the optimum β angle in real-time experiments. Fig. 8 illustrates the proposed MTPA flowchart. As can be seen from Fig. 8, the proposed LuT-based MTPA method determines the MTPA points by identifying the points at which the electromagnetic torque is maximum. Hence, the proposed approach has been implemented as a simple and effective solution.

IV. EXPERIMENTAL RESULTS

The test setup created to represent an electric vehicle is given in Fig. 9. The DC power supply provides the necessary energy for the drive system, which represents the vehicle's battery pack. The drive is controlled by a dSpace 1202 microprocessor that implements the FOC strategy to control the IPMSM. The inverter is switched using the SVPWM technique with an 8 kHz switching frequency, providing high dynamic response and low harmonic distortion. The dyno mounted to the machine in Fig. 9 generates the load torque, and the speed of the machine varies based on the difference between the electromagnetic torque and the mechanical load. Since torque control is performed, the dyno is used manually. That is, the load setting is adjusted according to the desired speed. A blower is for cooling down the dynamometer. A voltage source inverter is the power electronics for the conversion of DC energy into AC and feeding the AC machine. An optocoupler achieves the isolation between the controller and the inverter, and it is used for voltage level shift as well. This is required in the test system since the controller provides digital output with a maximum voltage of 5 V, while the inverter requires 18 V. An uninterruptible power supply is employed for the protection of equipment in case of power failure. The dyno controller is employed

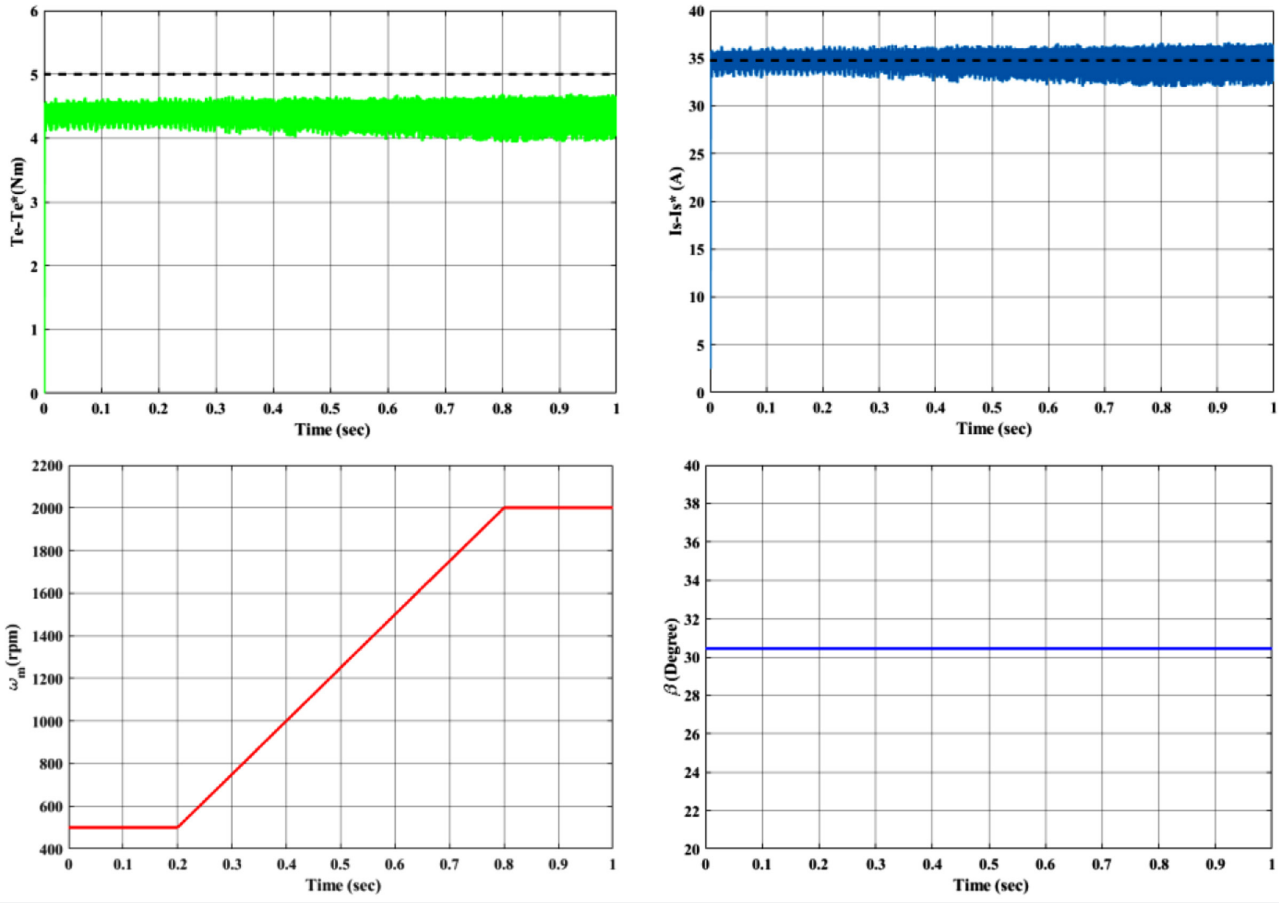

Fig. 7. Parameter dependency of conventional drive at 5 Nm reference torque.

as a voltage-controlled current source, where 0 A corresponds to no load, while 3 A achieves full load capacity of the dyno, which is around 32 Nm. The test setup consists of three current sensors mounted on the inverter, a torque sensor, and an encoder for speed and position angle measurement. During torque measurement, a low-pass filter has been applied to obtain smooth and reliable results. This setup enables real-time testing of IPMSM performance under controlled conditions that closely resemble the operating environment of an electric vehicle, allowing for accurate evaluation of torque, current, and speed behavior.

The β sweep procedure is structured such that the angle increases by 1° per 2 seconds, resulting in a total increase of 45° over the 90-second operating period. This setup allows real-time observation of the machine's response under controlled β variations, ensuring accurate determination of MTPA points by accounting for the system's dynamic behavior. The computed –dq axis current values have been stored in lookup tables, and linear interpolation has been employed for intermediate value estimation. To design the proposed drive, the stator current magnitude has been kept constant during the tests, and the current angle β has been linearly increased from 0° to 45° with a constant slope. Meanwhile, the mechanical speed of the machine has been kept below 2000 rpm with the help of a brake (the mechanical load-dyno). By repeating the tests for each stator current magnitude value (10, 15, 20, 25, 30, 35, and 40 A), the –dq axis currents at which the maximum torque is produced have been recorded. It is noteworthy to remind that the torque maximization at constant stator current magnitude ensures the efficiency optimized control in the constant torque region and, as can be deduced from (14), this optimization is achieved regardless of the machine speed. Thus, the recorded optimum –dq axis currents by the proposed approach consider both the machine and the power electronics-based system variations into account, since the optimum current angle is obtained through online tests.

Fig. 10 gives an example of obtaining lookup table data when $I_s = 15$ A. T_{e_Actual} represents the actual torque of the machine measured from the torque transducer. It is noteworthy that the actual torque has been filtered by a low-pass filter. Similarly, throughout the study, the actual torque has been plotted using the same filter. $\check{T}_e$ represents the estimated torque by (7) where nominal machine parameters listed in are employed. As can be seen, the two torques are not the same, and this implies that the machine parameters deviate from their nominal values and, in practice, these variations need to be considered to achieve optimized control. Additionally, machine input-output powers, efficiency, –dq axis voltage vector as well as the voltage magnitude, the sector in which the voltage vector lies in (for SVPWM implementation), duty cycles for each phase, the mechanical speed in rpm, electrical rotor position angle, –dq and abc phase currents, and deliberately altered current angle are all illustrated in Fig. 10, and as can be seen, the actual state variables track the references accurately. The tests are carried out for different

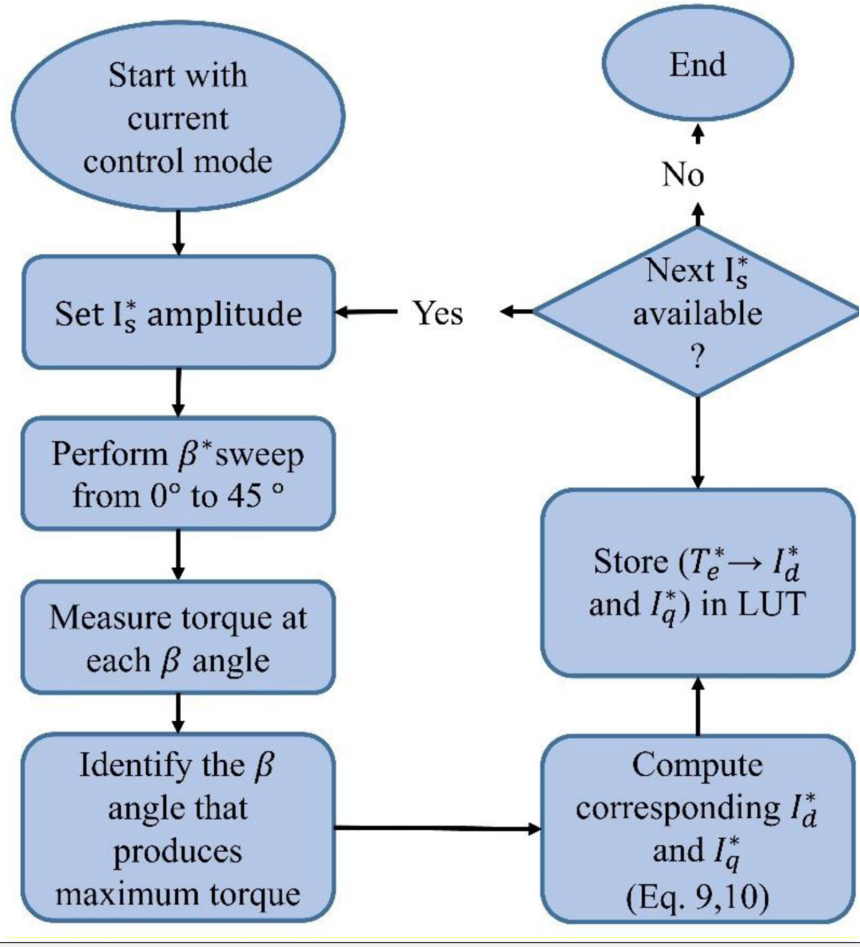

Fig. 8. Lookup table preparation for proposed maximum torque per ampere strategy.

stator current magnitudes, and actual torque responses are recorded in the proposed strategy. Then, the optimum current angle for different operating points is obtained and recorded, considering system nonlinearities.

Fig. 11 shows the torque control results of the MTPA technique on the test system with the conventionally used Newton–Raphson solution employing the conventional equation in (14). As mentioned, the Newton–Raphson technique can be used as an online mathematical solution method, or the electromagnetic torque corresponding to the –dq axis currents obtained for the ideal machine can be provided as a lookup table (in Fig. 5). The key to this paper is the comparison of the proposed real-time MTPA strategy with the conventional technique. A torque command of 1–5 Nm with a step of 1 Nm is demanded from the drive, and the robustness of the drive system is tested with the conventional strategy. The mechanical speed is kept below ~1000 rpm with the help of a brake, since increased electromagnetic torque increases the speed. The input-output powers, efficiency, voltage values, reference and measured –dq axis currents, 3-phase currents, mechanical speed, and stator current magnitude are all presented in Fig. 11. As can be seen, the reference I_d and I_q currents produced by the Newton–Raphson-based MTPA strategy are followed correctly by the actual currents, and the current errors are driven to zero. However, it is clear from the results that a gap occurs between the actual torque and the command torque. This is due to the fact that the actual machine parameters during operation deviate from those employed in the controller, and the drive system cannot achieve the demanded torque, leading to significant performance deterioration. The issue is sorted by the proposed approach, and the results are presented in Fig. 12.

Fig. 12 shows the drive results where the proposed approach is applied, and the same variables are shown in Fig. 12 as in Fig. 11. The electromagnetic torque demanded from the system is the same as in Fig. 11, and similarly, the mechanical speed is kept below ~1000 rpm with the help of a brake. Clearly, the torque value demanded from the drive system is met by the machine, and the performance is much improved. Hence, it is evident that the recorded data through online tests and employing them with the proposed approach as a simple and quite effective strategy significantly improves the system operation. 1–5 Nm torque commands correspond to -d axis currents obtained using the conventional MTPA method, which are –2, –6, –10.5, –14, and –17. 5 A, while in the proposed method, these values are higher, occurring as –3.5, –8, –13.5, –16.5, and –20 A. Similarly, while the -q axis currents in the conventional method were 8.5, 15.5, 21, 25, and 30 A, they were measured at 13, 18, 22, 26, and 31.5 A in the proposed method. These data statistically demonstrate that the proposed method provides a significant improvement over conventional MTPA, particularly in the low and medium torque regions, by more effectively utilizing the –d axis and –q axis currents in torque

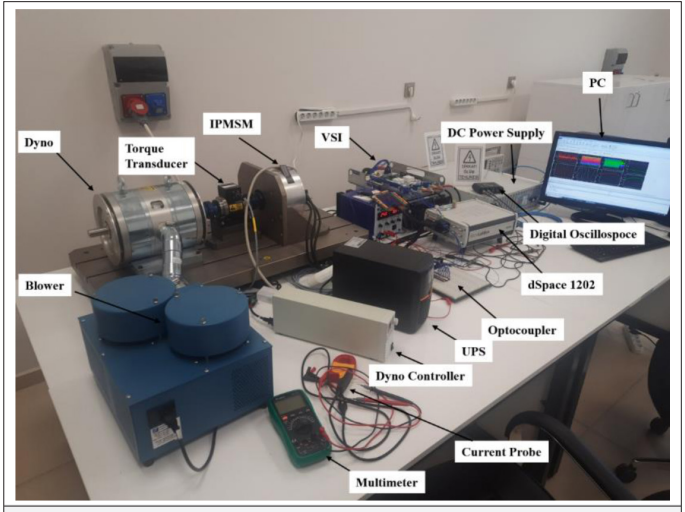

Fig. 9. Test rig.

generation. When analyzing the situation at 5 Nm command torque, the recommended drive can correctly generate 5 Nm command electromagnetic torque, while the drive using conventional MTPA generates approximately 4.6 Nm of torque. As a result, a torque gap of 0.4 Nm occurs, and the command torque cannot be met. Increasing current values according to the torque demanded by the system will dominate the variability in machine parameters. Therefore, a larger torque gap can be expected at higher current and torque values.

V. CONCLUSION

The necessity of applying torque control in electric vehicles and the importance of optimized torque control for high efficiency operation at accurate operating points have been discussed in this paper. It is emphasized that in order to achieve accurate torque control, the current commands to be generated from the torque command need to be obtained accurately in the IPMSM drives. It has been shown that the conventional drives significantly suffer from model dependency, and hence obtaining optimum current angle is a challenge for IPMSM

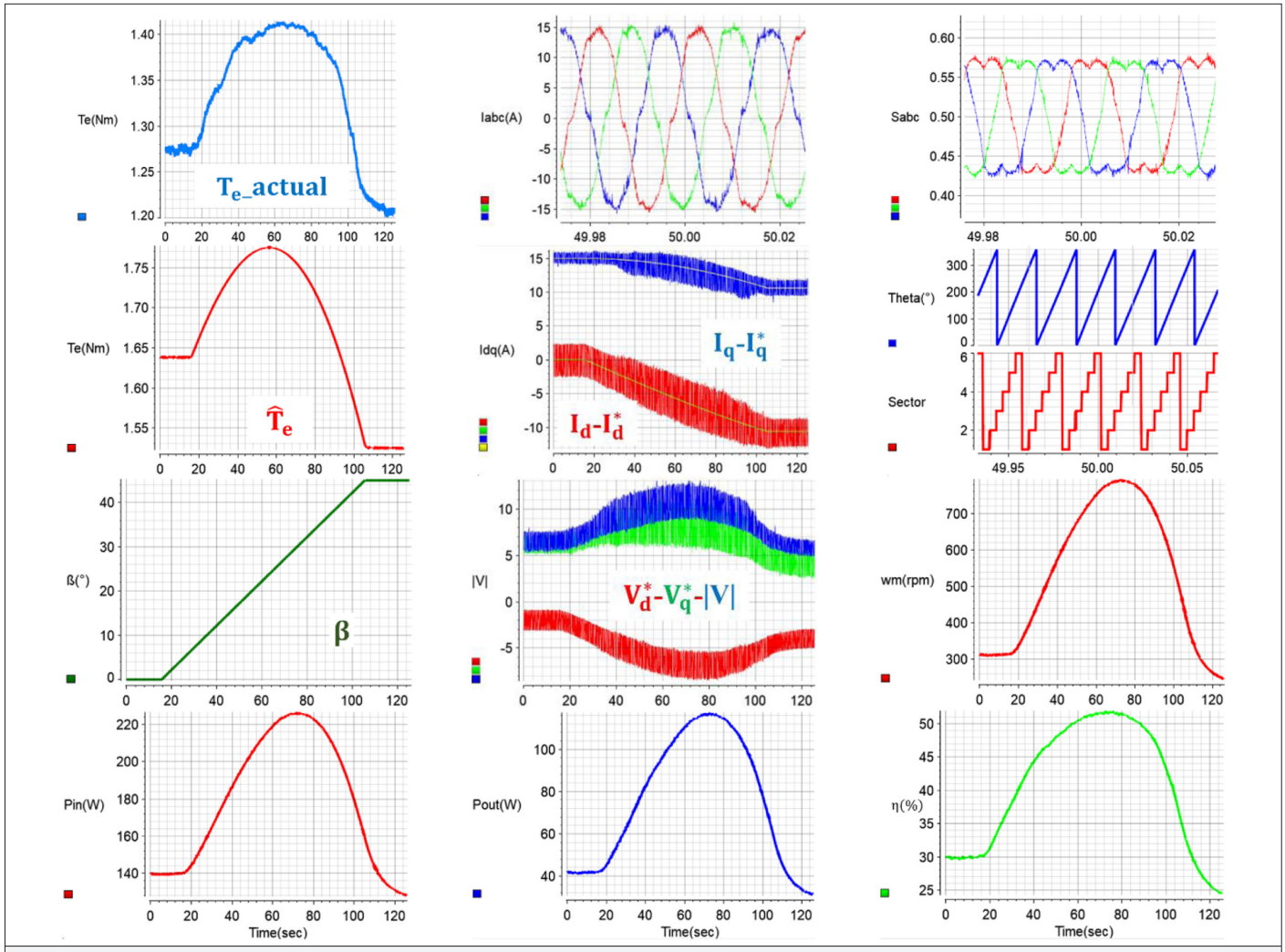

Fig. 10. Lookup table preparation for 15 A stator current magnitude test procedure to obtain optimum current angle for a given current magnitude.

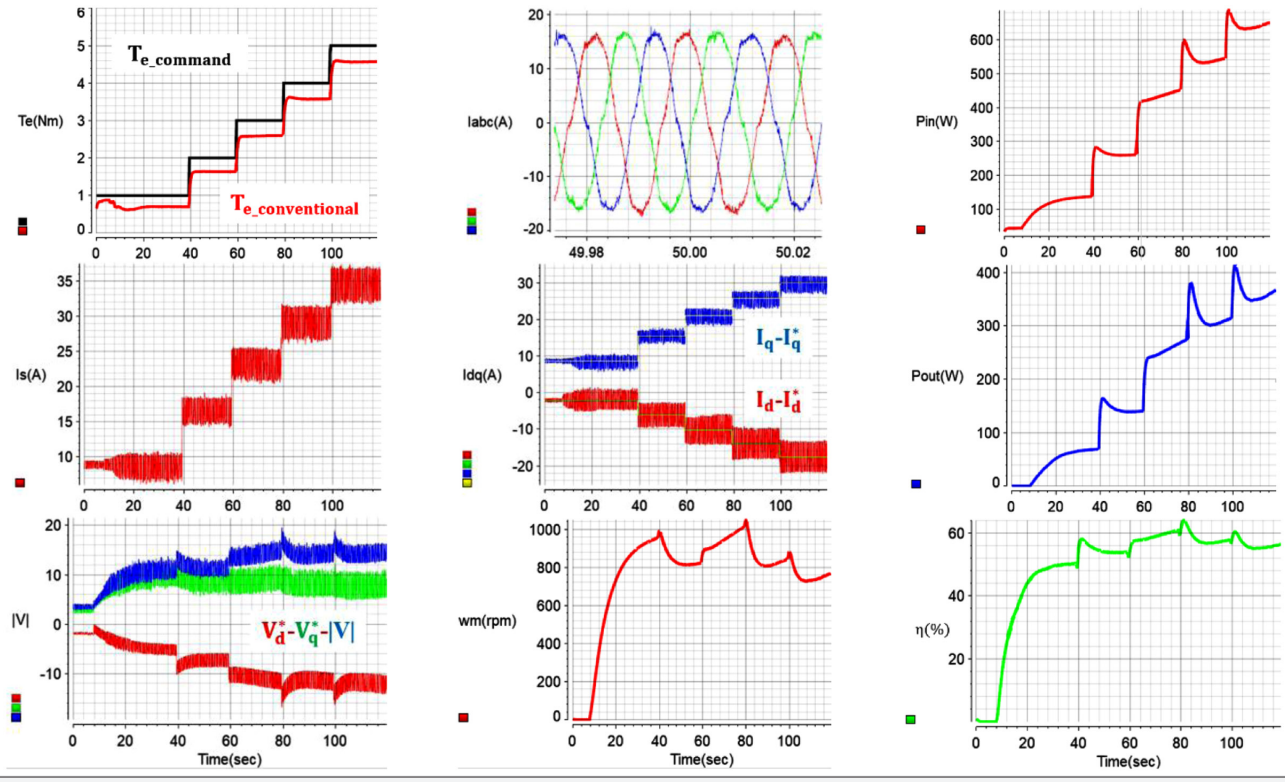

Fig. 11. Experimental results with the conventional maximum torque per ampere strategy.

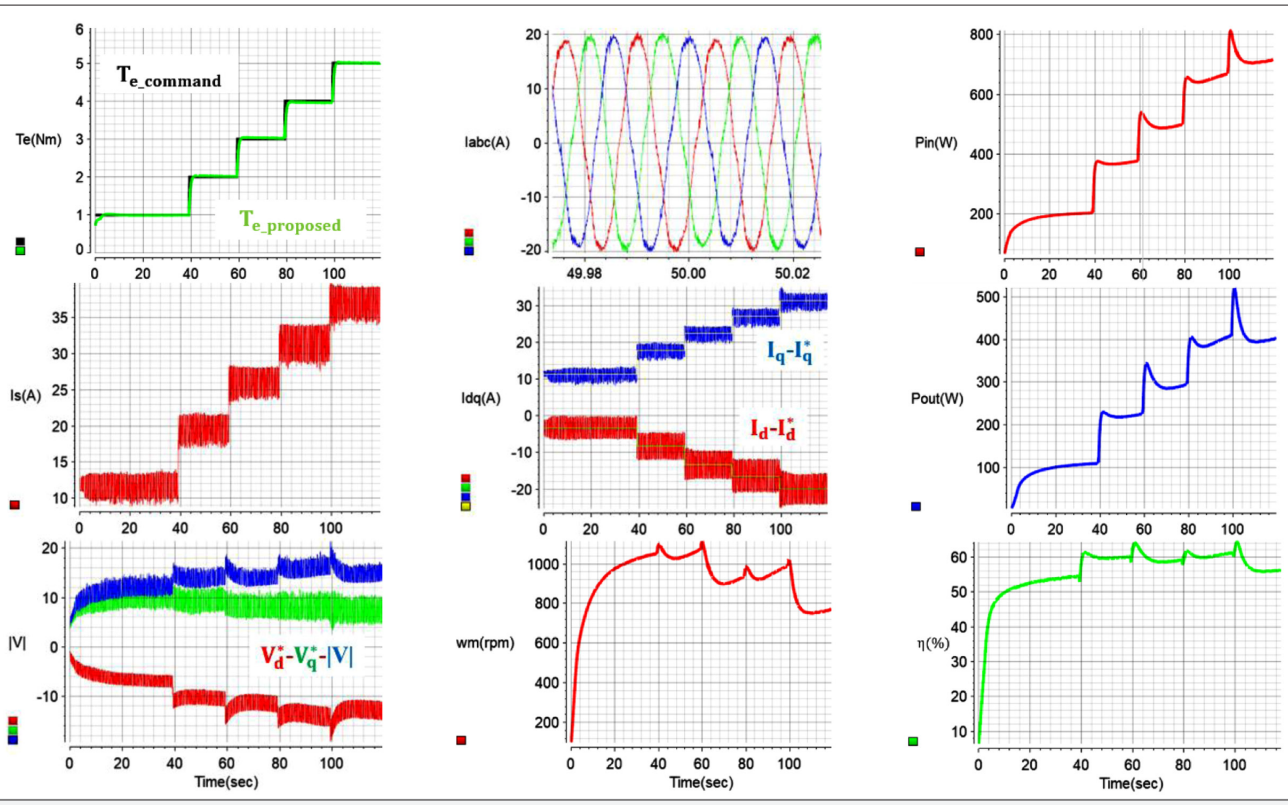

Fig. 12. Experimental results with the proposed maximum torque per ampere strategy.

drives where system nonlinearities are quite significant. From this perspective, experimental procedures have been improved where the optimum data have been recorded through online tests. It has been validated by simulation and experimental results that the generation of accurate current commands considering machine parameter variations as well as experimental drive system nonlinearities much improves the drive system performance. The proposed approach is quite simple and offers an effective solution to issues associated with a great number of modern drives, such as convergence problems of search-based drives, high computational burden issues of online numerical solutions–based drives, acoustic noise, increased current harmonics, and hence undesired torque ripples issues of signal injection-based drives. Therefore, the strategy can be simply adopted to IPMSM drives, and the drive performance can be significantly improved by avoiding the aforementioned issues as well.

Data Availability Statement: The data that support the findings of this study are available on request from the corresponding author.

Peer-review: Externally peer-reviewed.

Author Contributions: Concept – O.E.Ö.; Design – O.E.Ö.; Supervision – M.K., S.B.; Resources – M.K.; Materials – O.E.Ö., M.K.; Data Collection and/or Processing – O.E.Ö.; Analysis and/or Interpretation – O.E.Ö., M.K., S.B.; Literature Search – O.E.Ö.; Writing – O.E.Ö.; Critical Review – M.K., S.B.

Declaration of Interests: The authors declared that this study has received no financial support.

Funding: The research work was conducted with the financial supports of Scientific and Technological Research Council of Turkey (TUBITAK) through the Scientific and Technological Research Projects Funding Program (1001) with a project numbered as 118E858. Also, this study was supported by TUBITAK"s 2211-A scholarship program under the application number 1649B032205045.

REFERENCES

1. M. Koc, S. Emiroglu, and B. Tamyürek, "Analysis and simulation of efficiency optimized IPM drives in constant torque region with reduced computational burden," *Turk J. Elec Eng. Comp Sci.*, vol. 29, no. 3, pp. 1643–1658, 2021. [CrossRef]
2. Z. Wang, T. W. Ching, S. Huang, H. Wang, and T. Xu, "Challenges faced by electric vehicle motors and their solutions," *IEEE Access*, vol. 9, pp. 5228–5249, 2021. [CrossRef]
3. A. Aroua *et al.*, "Impact of scaling laws of permanent magnet synchronous machines on the accuracy of energy consumption computation of electric vehicles," *eTransportation*, Vol. 18, 2023/10/01/ 2023, p. 100269.
4. E. A. Grunditz, T. Thiringer, J. Lindström, S. Tidblad Lundmark, and M. Alatalo, "Thermal capability of electric vehicle PMSM with different slot areas via thermal network analysis," *eTransportation*, Vol. 8, 2021/05/01/ 2021, p. 100107.
5. M. K. B. Boumegouas, E. Ilten, K. Kouzi, M. Demirtas, and B. M'hamed, "Application of a novel synergetic observer for PMSM in electrical vehicle," *Electr. Eng.*, vol. 106, no. 5, pp. 5507–5521, 2024/03/07. [CrossRef]
6. P. Roy, and A. Banerjee, "A study on performance parameters of three-level T-type inverter based PMSM drives for electric vehicles applications," *Electr. Eng.*, vol. 106, no. 2, pp. 1121–1134, 2024/04/01, 2024. [CrossRef]
7. S. Ranjan, M. Singh, and M. Sreejeth, "ANFIS-based resonant controller for mitigating torque ripples and addressing parametric variation in PMSM-driven electric vehicle," *Arab. J. Sci. Eng.*, vol. 50, No. 14, pp. 10869–10880, 2025/01/11. [CrossRef]
8. N. K. Saxena, "Reactive power optimization using firefly algorithm for dispersed electric vehicles charging stations in radial distribution system," *Electrica*, vol. 25, no. 1, pp. 1–13, 2025. [CrossRef]
9. S.Taa, and B. Mokhtari, "Proposal of an optimal control of an electric vehicle by combined FOC and DTC techniques," *Electrica*, vol. 24, no. 3, pp. 660–669, 2024. [CrossRef]
10. S. S. Badini, and V. Verma, "MRAS-based speed and parameter estimation for a vector controlled PMSM drive," *Electrica*, vol. 20, no. 1, pp. 28–40, 2020. [CrossRef]
11. D. Mohanraj, J. Gopalakrishnan, B. Chokkalingam, and L. Mihet-Popa, "Critical aspects of electric motor drive controllers and mitigation of torque ripple—Review," *IEEE Access*, vol. 10, pp. 73635–73674, 2022. [CrossRef]
12. R. Yao, "Online d-q axis inductance identification for IPMSMs using FEA-driven CNN," *Ain Shams Eng. J.*, vol. 15, no. 12, p. 103130, 2024/12/01/ 2024. [CrossRef]
13. O. E. Özçiflikçi, M. Koç, and S. Bahçeci, "Maximum Torque per Ampere Strategy in IPM Drives for Electric Vehicles," *El-Cezeri*, Vol. 8, September, 2021, pp. 1405–1415.
14. L. Jarzebowicz, K. Karwowski, and W. J. Kulesza, "Sensorless algorithm for sustaining controllability of IPMSM drive in electric vehicle after resolver fault," *Control Eng. Pract.*, vol. 58, pp. 117–126, 2017/01/01/ 2017. [CrossRef]
15. M. A. Hamida, J. de Leon, and A. Glumineau, "Experimental sensorless control for IPMSM by using integral backstepping strategy and adaptive high gain observer," *Control Eng. Pract.*, vol. 59, pp. 64–76, 2017/02/01/ 2017. [CrossRef]
16. I. Qureshi, and V. Sharma, "Wide speed Range and torque control of IPMSM with MTPA-MTPV field weakening control," *Arab. J. Sci. Eng.*, vol. 49, no. 12, pp. 15833–15848, 2024/12/01, 2024. [CrossRef]
17. S. Kim, and J. K. Seok, "Maximum voltage utilization of IPMSMs using modulating voltage scalability for automotive applications," *IEEE Trans. Power Electron.*, vol. 28, no. 12, pp. 5639–5646, 2013. [CrossRef]
18. K. Li, and Y. Wang, "Maximum torque per ampere (MTPA) control for IPMSM drives using signal injection and an MTPA control law," *IEEE Trans. Ind. Inform.*, vol. 15, no. 10, pp. 5588–5598, 2019. [CrossRef]
19. W. Zhang, F. Xiao, J. Liu, Z. Mai, and C. Li, "Maximum torque per ampere control for IPMSM traction system based on current angle signal injection method," *J. Electr. Eng. Technol.*, vol. 15, no. 4, pp. 1681–1691, 2020/07/01, 2020. [CrossRef]
20. K. Li, T. Sun, J. Liang, M. Koc, and Y. Zhou, "Automatic MTPA control for IPMSM drives based on pseudorandomly reversed fixed-frequency sinusoidal signal injection," *IEEE Trans. Ind. Electron.*, pp. 1–12, 2023.
21. X. Liu, and Y. Du, "Torque control of interior permanent magnet synchronous motor based on online parameter identification using sinusoidal current injection," *IEEE Access*, vol. 10, pp. 40517–40524, 2022. [CrossRef]
22. T. Sun, J. Wang, and M. Koc, "On Accuracy of Virtual Signal Injection based MTPA Operation of Interior Permanent Magnet Synchronous Machine Drives," *IEEE Trans. Power Electron.*, vol. 32, no. 9, pp. 7405–7408, 2017. [CrossRef]
23. T. Sun, M. Koç, and J. Wang, "MTPA control of IPMSM drives based on virtual signal injection considering machine parameter variations," *IEEE Trans. Ind. Electron.*, vol. 65, no. 8, pp. 6089–6098, 2018. [CrossRef]
24. Y. Lu, S. He, C. Li, H. Luo, H. Yang, and R. Zhao, "Online full-speed region control method of IPMSM drives considering cross-saturation inductances and stator resistance," *IEEE Trans. Transp. Electrif.*, vol. 9, no. 2, pp. 3164–3176, 2023. [CrossRef]
25. X. An, G. Liu, Q. Chen, W. Zhao, and X. Song, "Adjustable model predictive control for IPMSM drives based on online stator inductance identification," *IEEE Trans. Ind. Electron.*, vol. 69, no. 4, pp. 3368–3381, 2022. [CrossRef]
26. N. lu, "MTPA trajectory tracking control with on-line MRAS parameter identification for an IPMSM," *J. Electr. Eng. Technol.*, vol. 14, no. 6, pp. 2355–2366, 2019/11/01, 2019. [CrossRef]
27. M. Koç, and O. E. Özçiflikçi, "Precise torque control for interior mounted permanent magnet synchronous motors with recursive least squares algorithm based parameter estimations," *Eng. Sci. Technol. An Int. J.*, vol. 34, p. 101087, 2022/10/01/ 2022. [CrossRef]
28. M. Alzayed, H. Chaoui, and Y. Farajpour, "Dynamic direct voltage MTPA current sensorless drives for interior PMSM-based electric vehicles," *IEEE Trans. Veh. Technol.*, vol. 72, no. 3, pp. 3175–3185, 2023. [CrossRef]
29. M. Alzayed, and H. Chaoui, "Direct voltage MTPA speed control of IPMSM-based electric vehicles," *IEEE Access*, vol. 11, pp. 33858–33871, 2023. [CrossRef]
30. M. Khayamy, and H. Chaoui, "Current sensorless MTPA operation of interior PMSM drives for vehicular applications," *IEEE Trans. Veh. Technol.*, vol. 67, no. 8, pp. 6872–6881, 2018. [CrossRef]
31. H. Chaoui, M. Khayamy, and O. Okoye, "MTPA based operation point speed tracking for PMSM drives without explicit current regulation,"

Electr. Power Syst. Res., vol. 151, pp. 125–135, 2017/10/01/ 2017. [CrossRef]
32. C. Lai, G. Feng, J. Tjong, and N. C. Kar, "Direct calculation of maximum-torque-per-ampere angle for interior PMSM control using measured speed harmonic," *IEEE Trans. Power Electron.*, vol. 33, no. 11, pp. 9744–9752, 2018. [CrossRef]
33. N.-Z. Jin, H.-C. Chen, D.-Y. Sun, Z.-Q. Wu, K. Zhou, and L. Zhang, "Virtual signal injection maximum torque per ampere control based on inductor identification," *Energies*, vol. 15, no. 13, 2022. [CrossRef]
34. M. H. Mahmud, Y. Wu, and Y. Zhao, "Extremum seeking-based optimum reference flux searching for direct torque control of interior permanent magnet synchronous motors," *IEEE Trans. Transp. Electrif.*, vol. 6, no. 1, pp. 41–51, 2020. [CrossRef]
35. J. Lee, and J. W. Choi, "MTPA control method for MIDP SPMSM drive system using angle difference controller and P&O algorithm," *IEEE Trans. Power Electron.*, pp. 1–15, 2022.
36. S. Choi, W. Lee, A. Kang, S. Baek, and J. S. Lee, "Accuracy improvement of maximum torque per ampere control for interior permanent magnet synchronous motor drives reflecting PM flux linkage variations," *J. Power Electron.*, vol. 23, no. 11, pp. 1678–1687, 2023/11/01, 2023. [CrossRef]
37. S. Choi, and J. S. Lee, "Maximum torque per ampere control algorithm for an interior permanent magnet synchronous motor drive reflecting the PM flux linkage variations," *Presented at the IEEE Applied Power Electronics Conference and Exposition,* 2023. [CrossRef]
38. Z. Han, and J. Liu, "Comparative analysis of vibration and noise in IPMSM considering the effect of MTPA control algorithms for electric vehicles," *IEEE Trans. Power Electron.*, vol. 36, no. 6, pp. 6850–6862, 2021. [CrossRef]
39. O. E. Özçiflikçi, M. Koç, S. Bahçeci, and S. Emiroğlu, "Overview of PMSM control strategies in electric vehicles: A review," *Int. J. Dyn. Control*, vol. 12, No. 6, pp. 2093–2107, 2024. [CrossRef]
40. A. Dianov, F. Tinazzi, S. Calligaro, and S. Bolognani, "Review and classification of MTPA control algorithms for synchronous motors," *IEEE Trans. Power Electron.*, vol. 37, no. 4, pp. 3990–4007, 2022. [CrossRef]
41. A. Dianov, A. Anuchin, and A. Bodrov, "Robust MTPA control for steady-state operation of low-cost IPMSM drives," *IEEE J. Emerg. Sel. Top. Ind. Electron.*, vol. 3, no. 2, pp. 242–251, 2022. [CrossRef]
42. Z. Li, D. O'Donnell, W. Li, P. Song, A. Balamurali, and N. C. Kar, "A comprehensive review of state-of-the-art maximum torque per ampere strategies for permanent magnet synchronous motors," *Presented at the 10th International Electric Drives Production Conference (EDPC),* 2020. [CrossRef]
43. O. E. Özçiflikçi, and M. Koç, "Comparison of interior mounted permanent magnet synchronous motor drives with sinusoidal, third harmonic injection, and space vector pulse width modulation strategies in particular attention to current distortions and torque ripples," *Electrica*, vol. 23, no. 2, pp. 151–159, 2023. [CrossRef]
44. K. D. Hoang, P. Lazari, K. Atallah, J. G. Birchall, and S. D. Calverley, "Evaluation of simplified model for rapid identification and control development of IPM traction machines," *IEEE Trans. Transp. Electrif.*, vol. 7, no. 2, pp. 779–792, 2021. [CrossRef]
45. T. Sun, L. Long, R. Yang, K. Li, and J. Liang, "Extended virtual signal injection control for MTPA operation of IPMSM drives with online derivative term estimation," *IEEE Trans. Power Electron.*, vol. 36, no. 9, pp. 10602–10611, 2021. [CrossRef]

Osman Emre Özçiflikçi was born in Turkey. He received the BSc and MSc degrees from Erciyes University, Kayseri, Turkey, in 2019 and 2021, respectively, both in Electrical and Electronics Engineering, where he is currently pursuing the PhD degree. He is a Research Assistant in the Electrical and Electronic Engineering Department in the Engineering Faculty at Kirsehir Ahi Evran University. His research interests include electrical machines and AC drives.

Mikail Koç was born in Turkey. He received the BSc degree from ESOGU University, Eskisehir, Turkey, in 2009, the MSc degree from Nottingham University, Nottingham, UK, in 2012, and the PhD from the University of Sheffield, Sheffield, UK, in 2016, all in electrical and electronics engineering. He is currently an Associate Professor with the Engineering Faculty, Kirsehir Ahi Evran University, Kirsehir, Turkey. His research interests include advanced control strategies for AC drives.

Serkan Bahçeci was born in Turkey. He received the BSc degree from Yıldız Technical University, İstanbul, Turkey, in 2009, the MSc degree from Erciyes University, Kayseri, Turkey, in 2012, and the PhD degree from Erciyes University, Kayseri, Turkey, in 2017, all in electrical and electronics engineering. He is currently an Assistant Professor with the Engineering Faculty, Erciyes University, Kayseri, Turkey. His research interests include smart grid and electric power applications.